Site-Directed Mutagenesis of Conserved Charged Amino Acid Residues in ClpB from *Escherichia coli*[†,‡]

Micheal E. Barnett and Michal Zolkiewski*

Department of Biochemistry, Kansas State University, Manhattan, Kansas 66506

Received May 21, 2002; Revised Manuscript Received July 18, 2002

ABSTRACT: ClpB is a member of a multichaperone system in *Escherichia coli* (with DnaK, DnaJ, and GrpE) that reactivates strongly aggregated proteins. The sequence of ClpB contains two ATP-binding domains, each containing Walker consensus motifs. The N- and C-terminal sequence regions of ClpB do not contain known functional motifs. In this study, we performed site-directed mutagenesis of selected charged residues within the Walker A motifs (Lys212 and Lys611) and the C-terminal region of ClpB (Asp797, Arg815, Arg819, and Glu826). We found that the mutations K212T, K611T, D797A, R815A, R819A, and E826A did not significantly affect the secondary structure of ClpB. The mutation of the N-terminal ATP-binding site (K212T), but not of the C-terminal ATP-binding site (K611T), and two mutations within the C-terminal domain (R815A and R819A) inhibited the self-association of ClpB in the absence of nucleotides. The defects in self-association of these mutants were also observed in the presence of ATP and ADP. The four mutants K212T, K611T, R815A, and R819A showed an inhibition of chaperone activity, which correlated with their low ATPase activity in the presence of casein. Our results indicate that positively charged amino acids that are located along the intersubunit interface (this includes Lys212 in the Walker A motif of the N-terminal ATP-binding domain as well as Arg815 and Arg819 in the C-terminal domain) participate in intersubunit salt bridges and stabilize the ClpB oligomer. Interestingly, we have identified a conserved residue within the C-terminal domain (Arg819) which does not participate directly in nucleotide binding but is essential for the chaperone activity of ClpB.

ClpB belongs to the Hsp100 family of proteins (often termed Clp ATPases) (*1*, *2*), a subclass within the AAA^+ protein superfamily (*3*). AAA^+ proteins couple ATP hydrolysis with a variety of cellular functions that involve protein transport, protein unfolding, and dissociation of protein complexes (*4*). Among Clp ATPases, bacterial proteins, ClpA, ClpX, and ClpY (HslU), unfold protein substrates and deliver them to peptidases for degradation (*5*−*8*). In contrast, bacterial ClpB and yeast Hsp104 participate in multichaperone systems (with Hsp70 and Hsp40) that efficiently reactivate strongly aggregated proteins (*9*−*12*). The molecular mechanism of protein disaggregation and reactivation mediated by ClpB or Hsp104 is currently unknown.

A unifying structural property of all Clp ATPases is the formation of ring-shaped oligomers. ClpA, ClpX, HslU, Hsp104, and its mitochondrial isoform, Hsp78, assemble into hexamers (*13*−*17*). Intriguingly, electron microscopy image analysis indicates a 7-fold symmetry of ClpB oligomers (*18*). In solution, ClpB undergoes reversible self-association (*19*). Since ATP binds only weakly to monomeric ClpB and has a higher affinity for the oligomeric form, the self-association of ClpB is enhanced in the presence of ATP (*20*). Moreover, whereas the self-association of ClpB is strong in low-ionic strength buffers, the ClpB oligomers dissociate into monomers under high-ionic strength conditions (*18*). This indicates that electrostatic interactions between monomers play an important role in stabilizing the oligomeric form of ClpB.

The amino acid sequence of ClpB contains two nucleotide binding domains (NBDs; see Figure 1A) that are highly conserved among different Hsp100 proteins (*1*). The NBDs are enclosed between less conserved N- and C-terminal extensions and are separated with a middle linker region. Each of the NBDs contains Walker A, Walker B, and sensor 1 motifs, which have been found in all AAA^+ sequences (*3*). The N-terminal region of ClpB forms a distinct folding domain that does not contain known functional motifs; it is, however, essential for the in vitro chaperone activity of ClpB (*20*, *21*). The middle linker region is significantly longer in ClpB and Hsp104 than in ClpA. The function of the variable-length middle regions in Clp ATPases is currently unknown. The C-terminal region of ClpB contains the AAA sensor 2 motif (*3*), which supports the binding of nucleotides to NBD2 (*22*). Our previous studies have shown that the C-terminal domain of ClpB maintains intersubunit contacts that are necessary for the self-association of ClpB (*20*). The C-terminally truncated ClpB not only does not form oligomers but also has no ATPase activity and no chaperone activity either. These results indicate that the self-association of ClpB is essential for its biological function.

To further characterize the mechanism of stabilization of ClpB oligomers, we have focused on selected conserved

[†] This work was supported by National Institutes of Health Grant GM58626 and by the American Heart Association, Heartland Affiliate Grant 0060445Z.

[‡] This is contribution 02-440-J from the Kansas Agricultural Experiment Station.

* To whom correspondence should be addressed: Department of Biochemistry, 104 Willard Hall, Kansas State University, Manhattan, KS 66506. Phone: (785) 532-3083. Fax: (785) 532-7278. E-mail: michalz@ksu.edu.

10.1021/bi026161s CCC: $22.00
Published on Web 08/21/2002

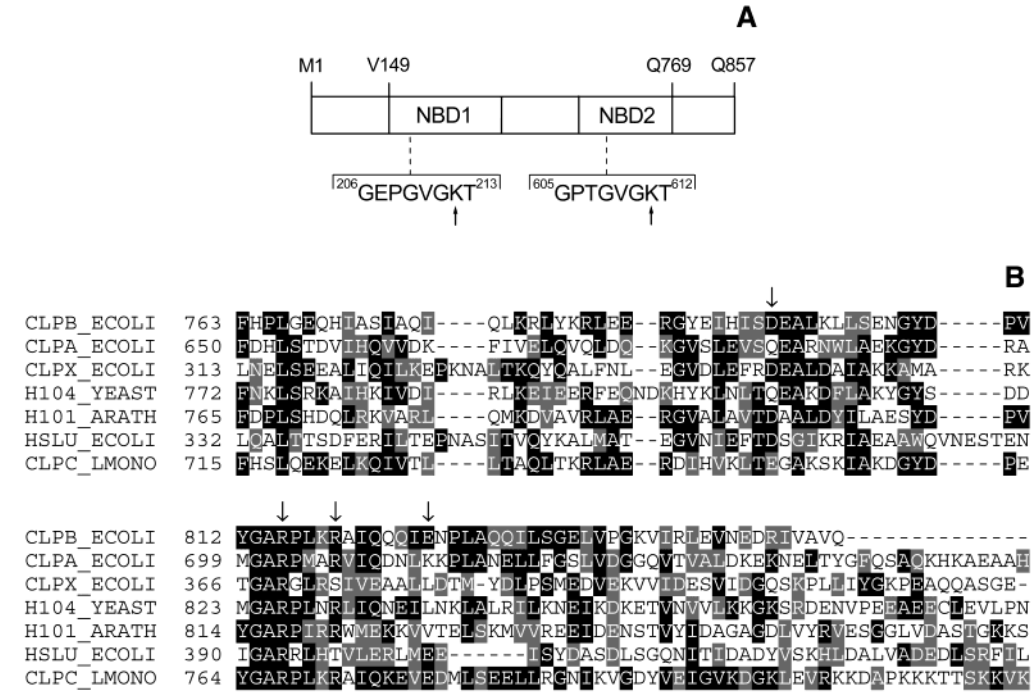

FIGURE 1: Postulated domain structure of ClpB and positions of mutations. (A) The diagram shows two nucleotide binding domains (NBD1 and NBD2) enclosed between the N-terminal and C-terminal regions and separated with the middle domain. Sequences of Walker A motifs within NBD1 and NBD2 are shown below, and the mutated lysine residues are denoted with arrows. (B) Sequence alignment of the C-terminal regions from seven Hsp100 proteins: ClpB from *E. coli*, ClpA from *E. coli*, ClpX from *E. coli*, Hsp104 from *Saccharomyces cerevisiae*, Hsp101 from *Arabidopsis thaliana*, HslU (ClpY) from *E. coli*, and ClpC from *Listeria monocytogenes*. The alignment was produced with T-COFFEE, version 1.37, and the output was created with Boxshade (http://www.ch.embnet.org). Identical matches and conservative substitutions are highlighted in black and gray, respectively. Arrows denote the amino acids in ClpB that were chosen for mutations.

charged residues in ClpB. We hypothesize that the removal of electric charges associated with specific amino acid side chains, which are located at the intersubunit interface, may destabilize the oligomeric ClpB and may inhibit its biochemical activity. In this work, we have performed site-directed mutagenesis of six charged amino acids in ClpB. Two of the chosen mutations, K212T and K611T, occur within Walker A nucleotide-binding motifs of NBD1 and NBD2, respectively (see Figure 1A). Mutations of these conserved lysines have been produced before for ClpB (*18*, *23*−*25*) and Hsp104/Hsp78 (*16*, *17*). Since the ATP-binding sites in ClpB are likely located at intersubunit interfaces (*15*, *20*), the conserved lysines may participate in stabilization of the oligomeric structure. However, in the previous work, the effects of lysine mutations were investigated in the context of ATP binding and hydrolysis, and the effects of these mutations on the oligomer stability itself have not yet been evaluated.

Four remaining mutations were introduced within the C-terminal domain of ClpB. As shown in Figure 1B, the sequence conservation among Clp ATPases in the C-terminal region is poor, with the exception of the highly conserved sensor 2 motif (Gly813−Pro816 in ClpB). In HslU, the only Clp ATPase with a published high-resolution structure, the α-helix between Gly391 and Ile406 is located at the surface of the C-terminal domain and is in contact with a neighboring subunit within the HslU hexamer (*15*). The α-helix in HslU contains several charged residues that expose their side chains to the intersubunit interface. In ClpB, we have selected for mutagenesis three charged residues in the corresponding sequence region: Arg815 (conserved arginine of the sensor 2 motif), Arg819, and Glu826. In addition, we have mutated Asp797, which is conserved among several Clp ATPases (see Figure 1B) and is exposed at the surface of the C-terminal domain of HslU (*15*). Each of the selected residues within the C-terminal domain of ClpB has been replaced with an alanine. We found that three of the selected charged residues (Lys212, Arg815, and Arg819) directly support the self-association of ClpB and that defects in quaternary structure of the mutants K212T, R815A, and R819A are further reflected in their low ATPase and chaperone activity.

EXPERIMENTAL PROCEDURES

Proteins. Site-directed mutagenesis was performed using the QuickChange method (Stratagene) with the plasmid pET-20b containing the ClpB sequence as the template (*20*). The following mutations have been introduced into the sequence of the ClpB gene: position 635, A → C (K212T); position 1832, A → C (K611T); position 2390, A → C (D797A); position 2443, C → G, and position 2444, G → C (R815A); position 2455, C → G, and position 2456 G → C (R819A); position 2477, A → C (E826A). The mutations were confirmed by the DNA sequencing facility at Iowa State University (Ames, IA).

Wild-type ClpB and the mutant proteins were overexpressed and purified as described previously (*20*). After purification, the proteins were dialyzed against 50 mM Tris-HCl (pH 7.5), 0.2 M KCl, 10% glycerol, 1 mM EDTA, and 1 mM DTT.[1] Protein concentrations were determined using an absorption coefficient A_{280}(0.1%) of 0.38 (in a 1 cm cuvette).

[1] Abbreviations: ClpBΔC, ClpB without the C-terminal domain; ClpBΔN, ClpB without the N-terminal domain (see ref *20*); DTT, dithiothreitol; HPLC, high-performance liquid chromatography.

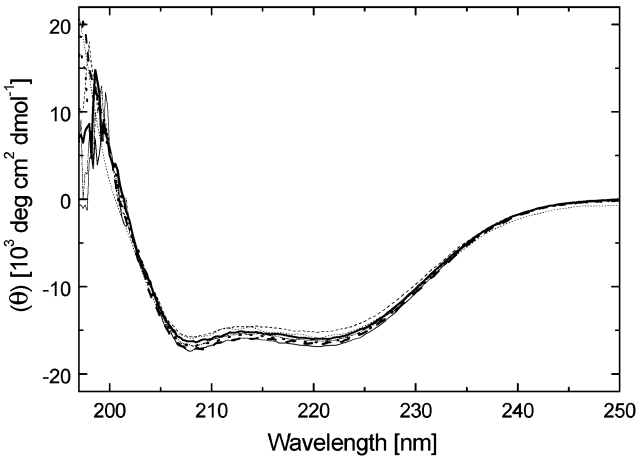

FIGURE 2: Far-UV circular dichroism (CD) spectra of ClpB and its mutant forms at room temperature. The CD signal is expressed as mean molar residue ellipticity (θ) and shown for wild-type ClpB (thick solid line), K212T (thick dashed line), K611T (thick dotted line), D797A (thin solid line), R815A (thin dashed line), R819A (thin dotted line), and E826A (dotted and dashed line). The protein concentration was 2.0 mg/mL in 50 mM Hepes-KOH (pH 7.5), 0.2 M KCl, 20 mM $MgCl_2$, 1 mM EDTA, and 2 mM β-mercaptoethanol.

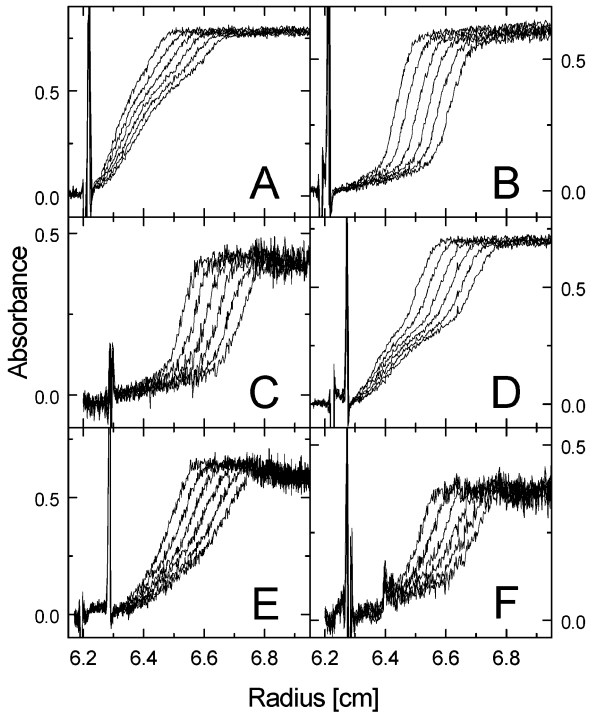

FIGURE 3: Sedimentation velocity of ClpB and its mutant forms. Ultracentrifugation was performed at 40 000 rpm and 20 °C. The protein concentration was 4.0 mg/mL in 50 mM Hepes-KOH (pH 7.5), 0.2 M KCl, 20 mM $MgCl_2$, 1 mM EDTA, and 2 mM β-mercaptoethanol. Protein concentration profiles were measured using absorption at 290 nm. Shown are radial scans of the centrifuge cell taken at 3 min intervals for K212T (A), K611T (B), D797A (C), R815A (D), R819A (E), and E826A (F). The direction of sedimentation is to the right, and the solution menisci are indicated by the light-scattering peaks at ~6.2−6.3 cm.

Firefly luciferase was purchased from Promega and κ-casein from Sigma. Other *Escherichia coli* chaperones (DnaK, DnaJ, and GrpE) were obtained from StressGen Biotechnologies (Victoria, BC).

Circular Dichroism. CD spectra were recorded with a Jasco J-720 spectropolarimeter at room temperature using a 0.02 cm cylindrical cell.

Analytical Ultracentrifugation. Sedimentation velocity experiments were carried out with a Beckman Optima XL-I analytical ultracentrifuge using two-channel cells with aluminum centerpieces, as described previously (*20*). The sedimentation velocity data were analyzed with the time-derivative method (*26*) using the software distributed with the instrument.

Gel Filtration Chromatography. Gel filtration experiments were performed using a Superose 6 PC 3.2/30 column (Amersham Pharmacia Biotech) with a Shimadzu HPLC system containing an LC-10ATvp solvent delivery unit and an SPD-M10Avp photodiode array detector. Gel filtration protein standards were obtained from Bio-Rad.

ClpB ATPase Activity Assays. Wild-type ClpB and the mutants (5 μg/mL) were incubated for 15 min at 37 °C in 100 mM Tris-HCl (pH 8.0), 10 mM $MgCl_2$, 5 mM ATP, 1 mM EDTA, 1 mM DTT, 0.1 mg/mL κ-casein, and either without or with 0.1, 0.2, or 0.3 M KCl. The inorganic phosphate concentration from ATP hydrolysis was measured using the malachite green assay (*27*, *28*).

Chaperone-Assisted Reactivation of Denatured Luciferase. Recombinant firefly luciferase was diluted into the unfolding buffer [30 mM Hepes-KOH (pH 7.6), 60 mM KCl, 10 mM $MgCl_2$, 1 mM EDTA, 10 mM DTT, and 7 M urea] and incubated for 30 min at room temperature. For refolding, the denatured luciferase was rapidly diluted 100-fold into the renaturation buffer [30 mM Hepes-KOH (pH 7.6), 120 mM KCl, 10 mM $MgCl_2$, 5 mM ATP, 1 mM EDTA, 1 mM DTT, and 0.1 mg/mL bovine serum albumin] containing wild-type ClpB or the mutants and the cochaperones DnaK, DnaJ, and GrpE. The activity of luciferase during refolding was determined as described previously (*10*).

RESULTS

To test the structural integrity of the ClpB mutants, we measured their circular dichroism (CD) spectra in the far-UV region (Figure 2). The CD spectra of wild-type ClpB and the mutants exhibit a negative band with a double minimum at 208 and 222 nm, which indicates a mostly α-helical structure. No apparent differences have been observed between the spectra of wild-type ClpB and the six mutants produced in this work, which indicates that the mutations do not affect the overall secondary structure of ClpB.

Since self-association of ClpB is necessary to support nucleotide binding, ATPase, and chaperone activity (*20*), we investigated the effects of mutations on the stability of ClpB oligomers (Figure 3). In a sedimentation velocity experiment, the rate of movement of a protein concentration boundary is related to the sedimentation coefficient of molecules in solution, whereas the shape of a boundary contains information about the homogeneity and diffusion properties of molecular species. In the buffer containing 0.2 M KCl, wild-type ClpB at a protein concentration of 4 mg/mL is fully associated and sedimentation velocity shows a single fast-sedimenting component (*20*). A similar sedimentation pattern has been observed for three ClpB mutants, K611T, D797A, and E826A (see Figure 3, panels B, C, and F). However,

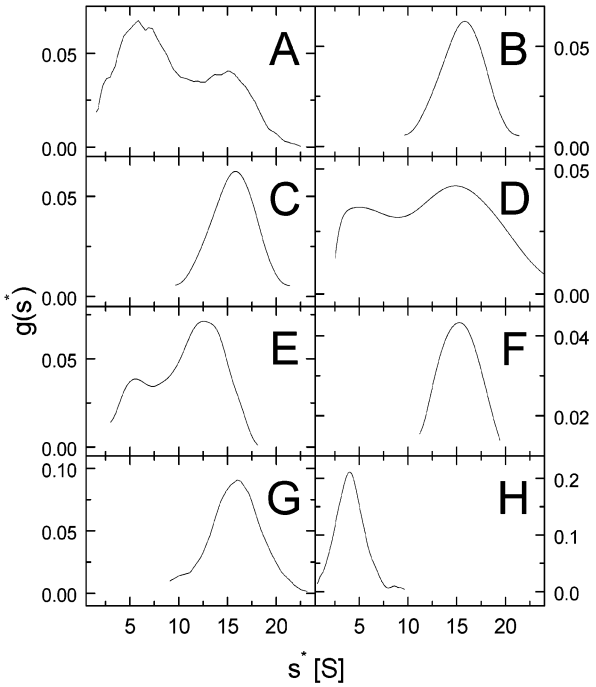

FIGURE 4: Apparent sedimentation coefficient distributions for ClpB and its mutant forms. Shown are the results of the time-derivative analysis (*26*) of four late protein concentration profiles (see Figure 3) for K212T (A), K611T (B), D797A (C), R815A (D), R819A (E), E826A (F), wild-type ClpB (G), and the C-terminally truncated ClpBΔC (H). The lines show apparent distribution functions $g(s^*)$ vs the sedimentation coefficient s^* in Svedbergs (S). The data for wild-type ClpB and ClpBΔC are from Barnett et al. (*20*).

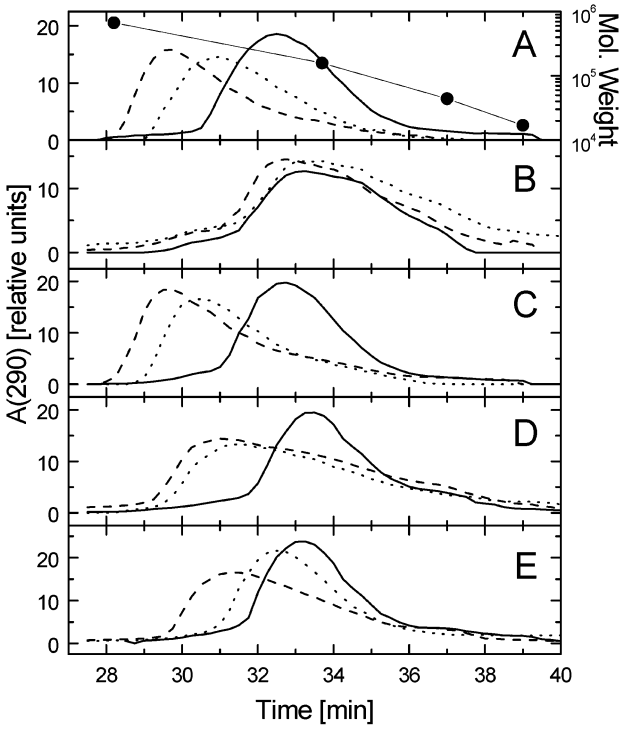

FIGURE 5: Gel filtration analysis of ClpB and its mutant forms in the presence of nucleotides. Aliquots of wild-type ClpB (A), K212T (B), K611T (C), R815A (D), and R819A (E) were injected onto a Superose 6 column (10 μL of 2.0 mg/mL protein). Protein elution profiles were obtained with a flow rate of 0.05 mL/min [running buffer consisting of 50 mM Tris-HCl (pH 7.5), 0.2 M KCl, 20 mM $MgCl_2$, 1 mM EDTA, and 1 mM DTT] in the absence of nucleotides (—), with 2 mM ATP in the running buffer (- - -), or with 2 mM ADP (•••) by monitoring absorption at 290 nm. Circles in panel A correspond to the elution times of thyroglobulin (M_r = 670 000), γ-globulin (M_r = 158 000), ovalbumin (M_r = 44 000), and myoglobin (M_r = 17 000). The data obtained with an analogous procedure for the mutants D797A and E826A are similar to those shown in panels A and C.

the heterogeneity of a solution was evident for three mutants, K212T, R815A, and R819A (see Figure 3, panels A, D, and E), where slow-sedimenting species were observed together with the fast-sedimenting oligomers.

Figure 4 shows the apparent sedimentation coefficient distributions [$g(s^*)$] for wild-type ClpB (panel G) and the mutants, obtained from the time-derivative analysis (*26*) of the data shown in Figure 3. In Figure 4, the s^* values corresponding to the maxima of the $g(s^*)$ distributions approximate the observed sedimentation coefficients of the species in solution. For comparison, the data for the C-terminally truncated ClpBΔC, which is monomeric and does not form oligomers (*20*), have been included in Figure 4H. It is evident that wild-type ClpB as well as K611T, D797A, and E826A fully associates into oligomers (Figure 4, panels B, C, F, and G). In contrast, the data for three mutants, K212T, R815A, and R819A (Figure 4, panels A, D, and E), indicate a high concentration of monomers in solution. We conclude that the self-association affinities of K212T, R815A, and R819A are lower than that of wild-type ClpB.

We next investigated whether the self-association defects of K212T, R815A, and R819A can be overcome in the presence of nucleotides. It has been shown before that ATP stabilizes the oligomeric form of ClpB from *E. coli* (*18*, *19*) and *Thermus thermophilus* (*24*, *25*). We used gel filtration chromatography to study the elution patterns of wild-type ClpB and the mutants in the absence of nucleotides and in the presence of ATP or ADP at a low protein concentration (~0.4 mg/mL) in the buffer containing 0.2 M KCl. As shown in Figure 5, wild-type ClpB and the mutants at low protein concentrations are not associated in the absence of nucleotides. ATP induces full self-association of wild-type ClpB (Figure 5A), as well as K611T (Figure 5C), D797A, and E826A (not shown). The oligomers do not fully assemble in the above protein samples in the presence of ADP. In contrast, neither ATP nor ADP induces full self-association of K212T, R815A, and R819A (Figure 5, panels B, D, and E). Defects of K212T, R815A, and R819A in the nucleotide-induced self-association mirror those observed in the absence of nucleotides in sedimentation velocity experiments. This result suggests that the mechanism of stabilization of the oligomeric ClpB by Lys212, Arg815, and Arg819 is nucleotide-independent and may simply involve charge−charge interactions of the amino acid side chains.

Our previous studies have shown a coupling between the self-association and the ATPase activity of ClpB (*20*). Whereas association deficient ClpBΔC cannot hydrolyze ATP, the enhanced self-association of ClpBΔN correlates with its increased basal rate of ATP hydrolysis. We investigated, therefore, the effects of mutations that destabilize oligomeric ClpB on its ATPase activity. Here, the role of specific amino acid residues in binding nucleotides and hydrolysis of ATP must be considered together with their effects on protein association. In the high-resolution structure of HslU, Lys63 of the Walker A motif interacts with the

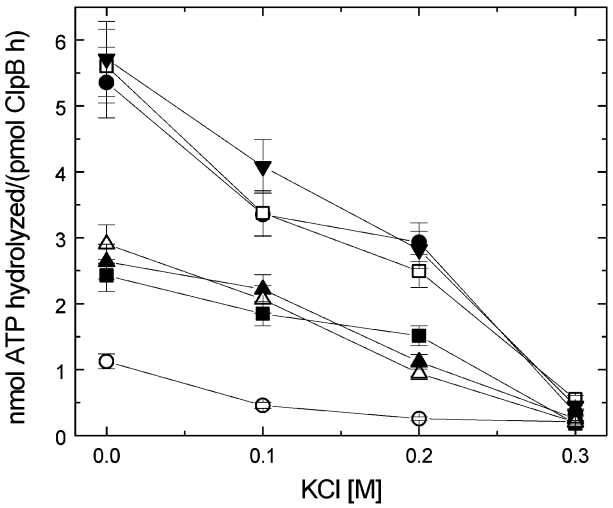

FIGURE 6: ATP hydrolysis by ClpB and its mutant forms. ATPase activity of ClpB was measured by incubating 5 μg/mL ClpB (●), K212T (○), K611T (■), D797A (□), R815A (▲), R819A (△), or E826A (▼) for 15 min at 37 °C in the assay buffer [100 mM Tris-HCl (pH 8.0), 10 mM $MgCl_2$, 5 mM ATP, 1 mM EDTA, 1 mM DTT, and 0.1 mg/mL κ-casein] with the indicated concentration of KCl.

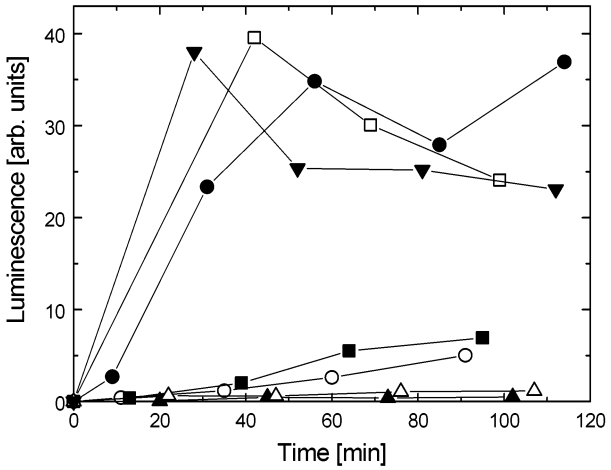

FIGURE 7: Reactivation of luciferase by ClpB and its mutant forms in the presence of DnaK, DnaJ, and GrpE. Unfolded luciferase was diluted at room temperature into the refolding buffer (see Experimental Procedures) containing DnaK, DnaJ, GrpE, and wild-type ClpB (●), K212T (○), K611T (■), D797A (□), R815A (▲), R819A (△), or E826A (▼). Luciferase activity was measured in aliquots withdrawn after the indicated times. Protein concentrations in the refolding solutions were as follows: 25 nM luciferase, 0.3 μM ClpB, 1.0 μM DnaK, 1.1 μM DnaJ, and 1.2 μM GrpE.

γ-phosphate of ATP (*15*). Due to a significant degree of sequence homology between Clp ATPases within the NBD regions, we can assume that Lys212 and Lys611 in ClpB are involved in similar interactions with ATP. A doubly mutated ClpB (K212T/K611T) has no ATPase activity, which suggests that single mutations K212T and K611T turn off the ATP hydrolysis within NBD1 and NBD2, respectively (*23*). In HslU, Arg393 of the sensor 2 motif also interacts with the β- and γ-phosphates of the nucleotide (*15*). Consistently, the sensor 2 Arg826 of Hsp104 directly supports binding of ATP and ADP (*22*), and we assume that Arg815 in ClpB may perform a similar function (see Figure 1B). In contrast, Asp797, Arg819, and Glu826 in ClpB correspond to the residues in HslU, which are not located in the vicinity of the nucleotide-binding site. Thus, we do not expect that these residues are involved in ATP binding.

Figure 6 shows the ATPase activity of ClpB in the presence of κ-casein. The ClpB ATPase is activated ~10-fold by casein (*20*, *29*). Results similar to those depicted in Figure 6 have been obtained in the absence of casein (not shown), but the accuracy of the measurements is better at the high ATP hydrolysis rate. As shown in Figure 6, the ATPase activity of ClpB decreases with an increasing salt concentration. This result agrees with those obtained previously for ClpB (*18*) and Hsp104 (*30*). The loss of ATPase activity in high-ionic strength buffers may be due to the decrease in self-association affinity of ClpB (*18*) as well as to yet uncharacterized inhibitory effects of salt on the ATP binding functions of ClpB.

Among the ClpB mutants produced in this work, D797A and E826A have the same ATPase activity as the wild type (Figure 6). This result agrees with similar self-association properties of D797A, E826A, and wild-type ClpB in the absence and presence of nucleotides. In contrast, K611T, the oligomerization of which is also similar to that of wild-type ClpB (see Figures 4 and 5), shows ~50% inhibition of the ATPase activity, which indicates an essential role of Lys611 in the ATP hydrolysis within NBD2 of ClpB. Two mutants, R815A and R819A, show extents of inhibition of the ATPase similar to that of K611T (Figure 6). Whereas Arg815 may be involved in binding ATP, Arg819 is most likely located outside the nucleotide-binding site. In contrast to K611T, both R815A and R819A show defects in self-association (Figures 4 and 5). Inhibition of the ATPase activity of R819A indicates that a loss of self-association propensity of this mutant may produce a loss of activity that is equivalent to that caused by removal of the essential Lys611. The mutant K212T shows the lowest ATPase activity among the ClpB variants (Figure 6). Like K611T, the K212T mutant does not contain the essential Walker A lysine, and the ATPase activity of NBD1 is expected to be low in K212T. In addition, unlike K611T, the K212T mutant shows a strong inhibition of self-association (Figures 4 and 5). The low ATPase activity of K212T may arise from a combined effect of the loss of the essential lysine and of the loss of nucleotide binding affinity in the partially dissociated ClpB.

Figure 7 shows the chaperone activity of the ClpB variants in the luciferase reactivation assay. As has been shown before, strong aggregation of luciferase during refolding prevents its spontaneous reactivation (*10*). Efficient recovery of the luciferase activity requires ClpB and three other *E. coli* chaperones: DnaK, DnaJ, and GrpE. Among the mutants produced in this work, D797A and E826A have the same chaperone activity as wild-type ClpB. This result correlates with no differences found for wild-type ClpB, D797A, and E826A in their quaternary structures and ATPase activities (see Figures 4 and 6). In contrast, the four remaining mutants show strong inhibition of the chaperone activity, which correlates with an inhibition of the ATPase of the same ClpB mutants (see Figures 6 and 7). Interestingly, the activities of R815A and R819A are the lowest among the ClpB variants shown in Figure 7.

DISCUSSION

In this study, we have compared the biochemical properties of wild-type ClpB and six mutants, each with a charged

amino acid substituted with an uncharged residue. We found that the mutations did not apparently affect the integrity of the secondary structure of ClpB (see Figure 2). However, in three of the mutants (K212T, R815A, and R819A), we observed significant defects in their quaternary structure (see Figures 3 and 4). The decrease in self-association affinity in the three mutants has been found in the absence of nucleotides as well as in the presence of ATP (see Figure 5). We conclude that positively charged side chains of the amino acids that are located along the intersubunit interface contribute to the stability of the ClpB oligomer through electrostatic interactions. This mechanism of oligomer stabilization includes Lys212 in the Walker A motif of NBD1, Arg815 in the sensor 2 motif, and Arg819 of the C-terminal domain. Our conclusion is in agreement with the previously observed dissociation of oligomeric ClpB in high-salt buffers (*18*) and may suggest a general mechanism of oligomer stabilization for other Clp ATPases and AAA^+ proteins. Interestingly, our results indicate that the roles of the conserved Lys212 in the Walker A motif and the conserved Arg815 in the sensor 2 motif are not limited to participation in nucleotide binding.

Several attempts were made in the past to assign specific functional roles to the two ATP-binding domains in Clp ATPases. In those studies, conserved Walker A motif lysines within NBD1 and NBD2 have been mutated and the effects of mutations on ATP-coupled functions (ATP-induced oligomerization and ATPase activity) have been investigated. It has been found that mutations within NBD1, but not NBD2, inhibit the ATP-induced association of bacterial ClpA (*31*) and ClpB (*18*, *25*). Thus, it has been tempting to define NBD1 as the ATP-binding structural module that couples nucleotide binding with protein self-association. In contrast, it has been observed that lysine mutations within NBD2, but not NBD1, inhibit the ATP-induced association of yeast proteins, Hsp104 and Hsp78 (*17*, *30*). It has been proposed that the functions of the two ATP-binding domains in Clp ATPases have been switched during the course of evolution between bacteria and yeast (*30*).

Our results help explain the above discrepancy by demonstrating that the effects of mutations within NBD1 and NBD2 on the self-association of ClpB should be considered independently from their ATP binding function. We have shown that Lys212, but not Lys611, is directly involved in stabilization of the ClpB oligomer, which manifests itself in the absence as well as in the presence of nucleotides (compare Figures 4 and 5). Most likely, whereas Lys212 participates in a salt bridge(s) with a negatively charged residue(s) from the neighboring ClpB subunit, Lys611 does not. Our conclusion is supported by an observation by Hattendorf and Lindquist that in Hsp104 it is the NBD2 lysine mutation that causes the loss of self-association affinity in the absence of nucleotides (*32*). Thus, the role of conserved Walker A lysines in the self-association of Clp ATPases is defined by the amino acid side chains that are located in the vicinity of the lysines within the oligomeric ring, rather than by the couplings between ATP binding and oligomerization that occur within a NBD. A similar intersubunit salt bridge involving a conserved glutamate of the Walker B motif has been found in the structure of p97, a AAA protein involved in membrane fusion (*33*). Our results demonstrate that removal of such intersubunit salt bridges strongly destabilizes the AAA oligomeric ring.

A unifying biochemical property of Clp ATPases is the nucleotide-induced protein self-association (*1*, *34*), also shown in this work for ClpB (see Figure 5). Structural studies of several members of the AAA^+ family documented conformational changes induced by nucleotide binding (*15*, *35*). Since the above results were based on the structure of oligomers, it is not known whether the nucleotide-induced conformational effects are responsible for nucleotide-induced self-association of the monomers. It has been suggested that the stabilization of oligomers by nucleotides may be due to the preferential binding of nucleotides to the oligomeric forms of Clp ATPases (*20*). Indeed, the affinity of binding of ATP to monomeric ClpB is very low (*20*). In such a case, the equilibrium between monomeric and oligomeric ClpB can be shifted toward the oligomer in the presence of a nucleotide according to the following equation (*36*):

$$K(L) = K(0)[P_o(L)/P_m(L)] \quad (1)$$

where L is the concentration of a nucleotide, $K(L)$ and $K(0)$ are the protein association equilibrium constants in the presence and absence of a nucleotide, respectively, and P_o and P_m are the binding polynomials of the protein oligomer and monomer, respectively. The value of a binding polynomial contains information about the nucleotide binding affinity of a given protein species. Preferential interaction of nucleotides with oligomeric ClpB implies that the ratio $P_o(L)/P_m(L) > 1$, which results in $K(L)$ being greater than $K(0)$ for either ATP or ADP (see Figure 5). From an incomplete assembly of oligomers in the presence of ADP (Figure 5A,C), one can deduce that ATP shows a stronger preference for oligomeric ClpB than ADP does. Consequently, ClpB may undergo partial dissociation−association cycles during ATP hydrolysis and rebinding.

The results of this work support the above thermodynamic model by demonstrating that, in a series of ClpB mutants, changes in the protein association affinity in the presence of nucleotides [$K(L)$] parallel those found in the absence of nucleotides [$K(0)$] (compare Figures 4 and 5). The mutations K212T, R815A, and R819A decrease the value of $K(0)$ and also decrease the value of $K(L)$, which is consistent with eq 1. The nucleotide-induced shifts in the protein self-association equilibrium can occur in parallel with yet-uncharacterized nucleotide-induced conformational changes in monomeric ClpB.

The two mutants, D797A and E826A, do not show a decrease in self-association affinity, as compared to the wild type, and have ATPase and chaperone activity similar to those of wild-type ClpB (Figures 6 and 7). This result indicates that Asp797 and Glu826 either are not located at the intersubunit interface in oligomeric ClpB or do not participate in essential intersubunit salt bridges. In contrast, the remaining four ClpB mutants show inhibition of both ATPase and chaperone activity. The defects in ATPase are likely due either to a decrease in self-association affinity, which results in a lower overall affinity for ATP (R819A), to a loss of an essential ATP-binding residue (K611T), or to both of the above mechanisms (K212T and R815A). It is striking that the mutation of Arg819, which is not likely a part of the ATP-binding site, produces a significant inhibition of the ClpB ATPase and a very strong inhibition of the

chaperone activity. It is possible that Arg819 plays an important, not yet characterized role in the chaperone activity of ClpB.

Although the mechanism of ClpB-mediated protein reactivation remains unknown, our results provide a link between the efficiency of oligomerization of ClpB and its chaperone activity (see Figure 7). A "molecular crowbar model" proposes that conformational changes in ClpB or Hsp104 may disrupt contacts between aggregated protein substrates (*2*, *9*). Our results raise a possibility that the cycle of association and dissociation of ClpB, which is driven by ATP binding and hydrolysis, may be partially responsible for inducing structural changes in aggregated proteins.

REFERENCES

1. Schirmer, E. C., Glover, J. R., Singer, M. A., and Lindquist, S. (1996) *Trends Biochem. Sci. 21*, 289−296.
2. Glover, J. R., and Tkach, J. M. (2001) *Biochem. Cell Biol. 79*, 557−568.
3. Neuwald, A. F., Aravind, L., Spouge, J. L., and Koonin, E. V. (1999) *Genome Res. 9*, 27−43.
4. Vale, R. D. (2000) *J. Cell Biol. 150*, F13−F19.
5. Weber-Ban, E. U., Reid, B. G., Miranker, A. D., and Horwich, A. L. (1999) *Nature 401*, 90−93.
6. Kim, Y. I., Burton, R. E., Burton, B. M., Sauer, R. T., and Baker, T. A. (2000) *Mol. Cell 5*, 639−648.
7. Singh, S. K., Grimaud, R., Hoskins, J. R., Wickner, S., and Maurizi, M. R. (2000) *Proc. Natl. Acad. Sci. U.S.A. 97*, 8898−8903.
8. Reid, B. G., Fenton, W. A., Horwich, A. L., and Weber-Ban, E. U. (2001) *Proc. Natl. Acad. Sci. U.S.A. 98*, 3768−3772.
9. Glover, J. R., and Lindquist, S. (1998) *Cell 94*, 73−82.
10. Zolkiewski, M. (1999) *J. Biol. Chem. 274*, 28083−28086.
11. Motohashi, K., Watanabe, Y., Yohda, M., and Yoshida, M. (1999) *Proc. Natl. Acad. Sci. U.S.A. 96*, 7184−7189.
12. Goloubinoff, P., Mogk, A., Zvi, A. P., Tomoyasu, T., and Bukau, B. (1999) *Proc. Natl. Acad. Sci. U.S.A. 96*, 13732−13737.
13. Kessel, M., Maurizi, M. R., Kim, B., Kocsis, E., Trus, B. L., Singh, S. K., and Steven, A. C. (1995) *J. Mol. Biol. 250*, 587−594.
14. Grimaud, R., Kessel, M., Beuron, F., Steven, A. C., and Maurizi, M. R. (1998) *J. Biol. Chem. 273*, 12476−12481.
15. Bochtler, M., Hartmann, C., Song, H. K., Bourenkov, G. P., Bartunik, H. D., and Huber, R. (2000) *Nature 403*, 800−805.
16. Parsell, D. A., Kowal, A. S., and Lindquist, S. (1994) *J. Biol. Chem. 269*, 4480−4487.
17. Krzewska, J., Konopa, G., and Liberek, K. (2001) *J. Mol. Biol. 314*, 901−910.
18. Kim, K. I., Cheong, G. W., Park, S. C., Ha, J. S., Woo, K. M., Choi, S. J., and Chung, C. H. (2000) *J. Mol. Biol. 303*, 655−666.
19. Zolkiewski, M., Kessel, M., Ginsburg, A., and Maurizi, M. R. (1999) *Protein Sci. 8*, 1899−1903.
20. Barnett, M. E., Zolkiewska, A., and Zolkiewski, M. (2000) *J. Biol. Chem. 275*, 37565−37571.
21. Tek, V., and Zolkiewski, M. (2002) *Protein Sci. 11*, 1192−1198.
22. Hattendorf, D. A., and Lindquist, S. L. (2002) *Proc. Natl. Acad. Sci. U.S.A. 99*, 2732−2737.
23. Kim, K. I., Woo, K. M., Seong, I. S., Lee, Z. W., Baek, S. H., and Chung, C. H. (1998) *Biochem. J. 333* (Part 3), 671−676.
24. Schlee, S., Groemping, Y., Herde, P., Seidel, R., and Reinstein, J. (2001) *J. Mol. Biol. 306*, 889−899.
25. Watanabe, Y. H., Motohashi, K., and Yoshida, M. (2002) *J. Biol. Chem. 277*, 5804−5809.
26. Stafford, W. F., III (1992) *Anal. Biochem. 203*, 295−301.
27. Hess, H. H., and Derr, J. E. (1975) *Anal. Biochem. 63*, 607−613.
28. Lanzetta, P. A., Alvarez, L. J., Reinach, P. S., and Candia, O. A. (1979) *Anal. Biochem. 100*, 95−97.
29. Woo, K. M., Kim, K. I., Goldberg, A. L., Ha, D. B., and Chung, C. H. (1992) *J. Biol. Chem. 267*, 20429−20434.
30. Schirmer, E. C., Queitsch, C., Kowal, A. S., Parsell, D. A., and Lindquist, S. (1998) *J. Biol. Chem. 273*, 15546−15552.
31. Singh, S. K., and Maurizi, M. R. (1994) *J. Biol. Chem. 269*, 29537−29545.
32. Hattendorf, D. A., and Lindquist, S. L. (2002) *EMBO J. 21*, 12−21.
33. Zhang, X., Shaw, A., Bates, P. A., Newman, R. H., Gowen, B., Orlova, E., Gorman, M. A., Kondo, H., Dokurno, P., Lally, J., Leonard, G., Meyer, H., van Heel, M., and Freemont, P. S. (2000) *Mol. Cell 6*, 1473−1484.
34. Gottesman, S., Maurizi, M. R., and Wickner, S. (1997) *Cell 91*, 435−438.
35. Rouiller, I., Butel, V. M., Latterich, M., Milligan, R. A., and Wilson-Kubalek, E. M. (2000) *Mol. Cell 6*, 1485−1490.
36. Wyman, J., and Gill, S. (1990) *Binding and Linkage. Functional Chemistry of Biological Macromolecules*, University Science Books, Mill Valley, CA.

BI026161S